

# A Generalized Multi-Frequency Impedance Matching Technique

M. A. Maktoomi<sup>1,2</sup>, R. Gupta<sup>1</sup>, M. H. Maktoomi<sup>1</sup>, M. S. Hashmi<sup>1,2</sup>, and F. M. Ghannouchi<sup>2</sup>

<sup>1</sup>Circuit Design Research Lab (CDRL), IIIT Delhi, New Delhi-110020, India

<sup>2</sup>Radio Lab, University of Calgary, Calgary, AB T2N1N4, Canada

Email: ayatullahm@iiitd.ac.in

**Abstract**— This paper describes a generalized multi-frequency impedance transformer capable of providing concurrent matching at arbitrary number of frequencies. A frequency dependent complex load (FDCL) has been considered but the scheme is applicable for real loads as well. The exact analysis of the proposed design results in closed form equations with many independent free variables to cater to the wide range of FDCLs. The proposed theory is validated through a prototype fabricated on Rogers RO5880, with permittivity of 2.2, and working at 0.9/1.8/2.1/2.9 GHz. The good agreement between measured and the EM simulated results validate the proposed technique.

## I. INTRODUCTION

A multi-frequency impedance matching network is a key component in majority of the multi-frequency RF/microwave components [1]. The literature is replete with reports on dual-frequency impedance transformers (DBITs) [2]-[7]. Some of these are useful for real load impedances [5], [7] whereas the others considered frequency dependent complex loads (FDCLs). Furthermore, [8] can be used for tri-frequency impedance matching for real load impedance; a systematic approach to design tri-frequency matching network valid for either type of loads was reported in [9]. All of the above mentioned design works at the number of frequencies they were intended for i.e. two and three, and they cannot be extended to higher number of frequencies. Two important works for multi-frequency impedance transformation technique were reported in [10]-[11]. Theoretically, there is no limitation on the number of frequencies that can be considered in [10]. However, design equation becomes more complicated as the number of frequencies is increased. In addition, [10] is valid for lumped elements that are not of much use at higher frequencies. On the other hand, formulations reported in [11] are not in closed form, and always require some optimization and search algorithm to arrive at a solution.

This paper, therefore, proposes a generalized technique to synthesize and design multi-frequency impedance matching network using distributed elements. Essentially, it builds upon the generic tri-frequency matching network reported in [9]. However, that approach cannot be directly extended to multi-frequency scenario, especially due to the use of open-circuited-short-circuited (OCSC) stub combination. An OCSC formulated as in [9] cannot work for more than two frequencies. This paper outlines the necessary modifications to facilitate such design. A quad-frequency matching network is



Fig. 1. Block level illustration of the proposed scheme.

analyzed, designed and fabricated to illustrate the underlying concepts; theoretically, there is no limitation on the number of frequencies or the type of load in the proposed technique. The exact analytical solution is provided to calculate the design parameters such as characteristic impedance and electrical length of the transmission lines and no optimization algorithm is required for a valid solution. The subsequent sections elaborate on the theoretical postulations and the prototype development followed by discussion on achieved results.

## II. THE PROPOSED IMPEDANCE TRANSFORMER

To illustrate higher level working of the proposed multi-frequency matching technique, a block diagram is shown in Fig. 1.  $Z_0$  and  $Z_L$  are the source and the load impedances. The dual-band impedance transformer (DBIT) establishes matching at the first two frequencies. Next, a dual-to-tri-band transformer (DTBT) is incorporated that establishes matching at the third frequency without affecting matching already achieved at the previous two frequencies. More details of DTBT can be referred from [9]. Similarly, a tri-to-quad-band transformer (TQBT) is used to achieve matching at the fourth frequency, and the TQBT must not disturb the matching already established at the previous three frequencies. It is apparent from this description that the scheme can be extended

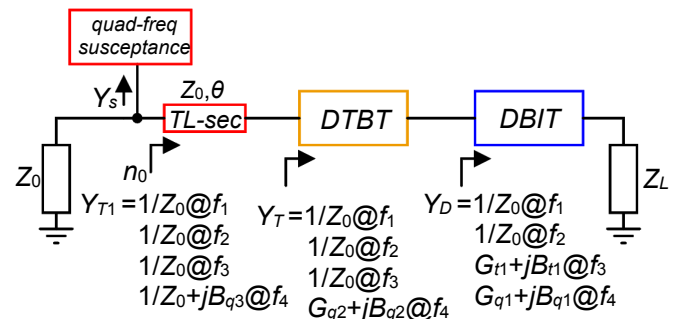


Fig. 2. Proposed quad-frequency impedance matching network.

to a penta-frequency impedance transformer by incorporating a quad-to-penta-band transformer (QPBT), and so on. Thus, theoretically, there is no restriction on the number of frequencies over which the proposed scheme can work.

#### A. Proposed Quad-Frequency Matching Network

The proposed quad-frequency impedance matching network is shown in Fig. 2. It is apparent from Fig. 2 that the proposed quad-frequency impedance transformer is a series connection of a dual-band impedance transformer (DBIT) [6], a dual-to-tri-band transformer (DTBT) [9], a transmission line (TL)-section", and a quad-frequency susceptance. As the load is frequency dependent, it is assumed to have distinct values at each frequency, namely,  $Z_L = R_1 + jX_1 @ f_1$ ,  $Z_L = R_2 + jX_2 @ f_2$ ,  $Z_L = R_3 + jX_3 @ f_3$ , and  $Z_L = R_4 + jX_4 @ f_4$ , and  $f_1 < f_2 < f_3 < f_4$ .  $Y_D$  represents the input admittance looking into the DBIT. Since, DBIT establishes matching at  $f_1$  and  $f_2$ , therefore  $Y_D = 1/Z_0 @ f_1$  and  $@ f_2$ .  $Y_D$ , in general, will have some complex value  $G_{11} + jB_{11} @ f_3$  and  $G_{q1} + jB_{q1} @ f_4$ . Similar comments can be made about  $Y_T$  and  $Y_{T1}$ —the input admittances looking into the DTBT and the TL-section, respectively. It must be noted that the TL-section and the quad-frequency susceptance constitutes the TQBT. Since,  $Y_T = 1/Z_0 @ f_1, @ f_2$  and  $@ f_3$ , therefore, the characteristic impedance of TL-section is selected as  $Z_0$ . Because of this choice matching is not disturbed at the first three frequencies. Moreover, the electrical length of the TL-section,  $\theta @ f_4$ , is determined such that  $\text{Re}(Y_{T1}) = 1/Z_0 @ f_4$ . Since, admittances sum at a junction, the imaginary part of  $Y_{T1}$  ( $=B_{q3}$ ) is to be cancelled at node  $n_0$  using a susceptance,  $Y_s$ . The susceptance must be a quad-frequency susceptance such that it adds zero susceptance at the first three frequencies, and  $-jB_{q3} @ f_4$ .

The schematic to realize a quad-frequency susceptance is shown in Fig. 3. This network is also used in multi-frequency DC-feed design [12]. In Fig. 3, the quad-frequency susceptance comprises of four cascaded L-networks for four frequency bands [12]. Each L-network constitutes of a transmission line (TL) section along with a quarter wavelength open stub. The terms " $Z_{it}$ " and " $\theta_i$ " is the characteristic impedance and electrical length of the  $i^{\text{th}}$  TL section, where as " $Z_{is}$ " and " $\theta_{is}$ " is the characteristic impedance and the electrical length of the  $i^{\text{th}}$  stub, with  $i=1, 2, 3, 4$ . All these electrical lengths are defined at the respective frequencies.

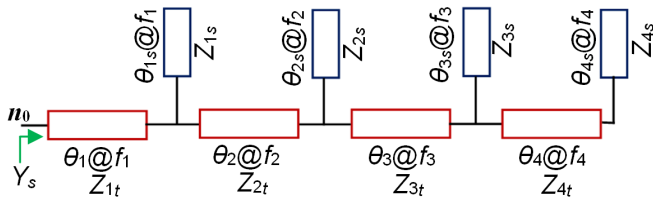


Fig. 3. The quad-frequency susceptance.

Now, the first three sections of the quad-frequency susceptance have been designed in such a way that it provides zero admittance looking into the node  $n_0$  at three frequencies  $f_1, f_2$ , and  $f_3$ , that is,  $Y_s = 0 @ f_1, @ f_2$  and  $@ f_3$ . Subsequently, the fourth L-network has been added to get the admittance term  $Y_s$ , expressed in (3), to cancel the imaginary part of  $Y_{T1}$ . The last two TL-sections in Fig. 3 can be combined together and the simplified expressions are given below.

$$Z_{4t} = Z_{4s} \quad (1)$$

$$\text{and} \quad \theta_{4t} = \theta_4 + \theta_{4s} \quad (2)$$

$$Y_s|_{f_4} = jY_{1t} * \left[ \frac{\tan(a_4 * 90) * (Y_{1s} + Y_{1t}) + Y_{2t} * \frac{A}{B}}{Y_{1t} - Y_{1s} * \tan^2(a_4 * 90) - Y_{2t} * \tan(a_4 * 90) * \frac{A}{B}} \right] \quad (3)$$

Where,  $a_i = f_i/f_1$ ,  $Y_{is} = 1/Z_{is}$ , and  $Y_{it} = 1/Z_{it}$  for  $i = \{1, 2, 3, 4\}$ . The terms  $A$  and  $B$  in (3) are given by expressions (4) and (5), mentioned at the bottom of this page.

### III. DESIGN PROCEDURE

A simplified sequence of design steps for the proposed matching network are summarized as follows:

- 1) **Step-I:** For a given load impedance, calculate the parameters of the DBIT. The calculations are referred from [6] here. This design should be validated through simulation.
- 2) **Step-II:** Design a tri-band impedance transformer [9]. Then validate the design again through simulation.
- 3) **Step-III:** Add a transmission line possessing characteristics impedance equal to the source impedance and with a variable electrical length. The electrical length must be varied in order to bring the real part of  $Y_{T1}$  ( $=G_{q2}$ ) equal to  $1/Z_0$ . Calculate the imaginary part of  $Y_T$  at  $f_4$ .
- 4) **Step-IV:** Design the first three sections of quad-frequency susceptance based on the technique used for multi-frequency DC feed network [12] and it must provide open at  $f_1, f_2$ , and  $f_3$ . Validate the design through simulation.
- 5) **Step-V:** Add 4<sup>th</sup> L-network to the quad-frequency susceptance and calculate  $Z_{4t}$  and  $\theta_{4t}$  from (1). Evaluate  $Y_{in} @ f_4$  from (3) and set  $Y_{in} @ f_4 = -jB_{q3}$ . It is now important to note that  $Z_{4t}$  or  $\theta_{4t}$  are also essentially a free variable here and this provides the proposed technique an additional degree of freedom.

### IV. DESIGN EXAMPLE AND DISCUSSION

A design example is considered here for four frequencies as follows:  $f_1 = 0.9$  GHz,  $f_2 = 1.8$  GHz,  $f_3 = 2.1$  GHz, and  $f_4 = 2.9$  GHz. A frequency dependent complex load is synthesized using a

$$A = Y_{2s} * \tan\left(\frac{a_4}{a_2} * 90\right) + Y_{2t} * \tan\left(\frac{a_4}{a_2} * \theta_2\right) + Y_{3t} * \left[ \frac{Y_{4t} * \tan\theta_4 + Y_{3s} * \tan\left(\frac{a_4}{a_3} * 90\right) + Y_{3t} * \tan\left(\frac{a_4}{a_3} * \theta_3\right)}{Y_{3t} - Y_{4t} * \tan\theta_4 * \tan\left(\frac{a_4}{a_3} * \theta_3\right) - Y_{3s} * \tan\left(\frac{a_4}{a_3} * 90\right) * \tan\left(\frac{a_4}{a_3} * \theta_3\right)} \right] \quad (4)$$

$$B = Y_{2t} - Y_{2s} * \tan\left(\frac{a_4}{a_2} * \theta_2\right) * \tan\left(\frac{a_4}{a_2} * 90\right) - Y_{3t} * \tan\left(\frac{a_4}{a_2} * \theta_2\right) * \left[ \frac{Y_{4t} * \tan\theta_4 + Y_{3s} * \tan\left(\frac{a_4}{a_3} * 90\right) + Y_{3t} * \tan\left(\frac{a_4}{a_3} * \theta_3\right)}{Y_{3t} - Y_{4t} * \tan\theta_4 * \tan\left(\frac{a_4}{a_3} * \theta_3\right) - Y_{3s} * \tan\left(\frac{a_4}{a_3} * 90\right) * \tan\left(\frac{a_4}{a_3} * \theta_3\right)} \right] \quad (5)$$

length of line and an SMD resistor. Variation of the real and imaginary parts of this FDCL is shown in Fig. 4, and it is found that  $Z_L = 43.97 + j22.39 @f_1$ ,  $57.62 + j45.73 @f_2$ ,  $65.71 + j53.43 @f_3$ , and  $101.59 + j68.17 @f_4$ .

As explained in Section III, the first step is to design DBIT and DTBT, which can be referred from [6], [9]. Their schematics are shown in Fig. 5. The electrical lengths and the characteristics impedances of the various transmission line sections of DBIT and DTBT are given in Table I. For clarity, it is reemphasized that the DBIT provides matching at the first two frequencies,  $f_1$  and  $f_2$ . Values of  $Y_D$  at the third and fourth frequency, that is,  $G_{r1} + jB_{r1} @f_3$  and  $G_{q1} + jB_{q1} @f_4$  are found to be as mentioned in Table II. The value at the third frequency is used to design DTBT that establishes matching at the third frequency [9]. Inclusion of DTBT provides matching at the first three frequencies of  $f_1$ ,  $f_2$ , and  $f_3$ . DTBT transforms  $G_{q1} + jB_{q1} @f_4$  into  $G_{q2} + jB_{q2} @f_4$ . It is apparent from Table III that real part of  $Y_T @f_4 (=G_{q2})$  is not equal to  $1/Z_0 = 0.02$ .

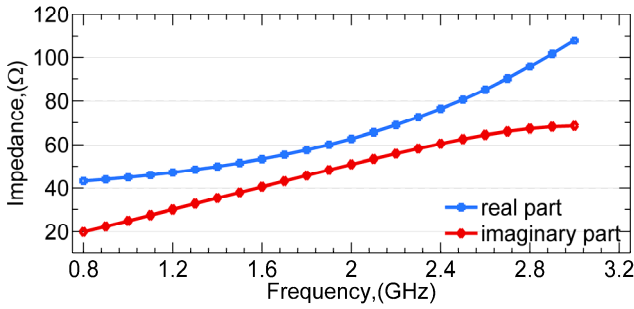


Fig. 4. Variation of the load impedance ( $Z_L$ ) with frequency.

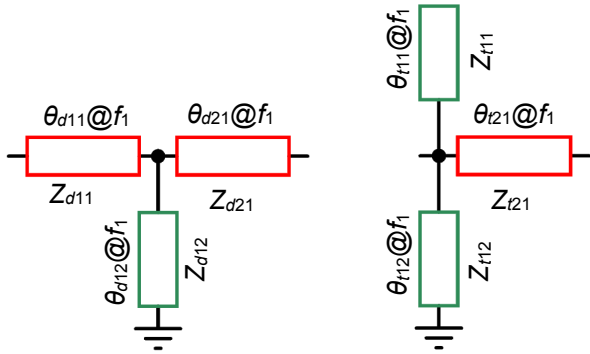


Fig. 5. Schematics of DBIT [6] and DTBT[9] used in this paper.

TABLE I. DESIGN PARAMETERS OF DBIT AND DTBT

Network	Impedance	value( $\Omega$ )	Electrical length	value( $^\circ$ ) @ $f_1$
DBIT	$Z_{d11}$	99	$\theta_{d11}$	60
	$Z_{d12}$	65.51	$\theta_{d12}$	120
	$Z_{d21}$	89.43	$\theta_{d21}$	39.18
DTBT	$Z_{t11}$	65.8	$\theta_{d11}$	60
	$Z_{t21}$	21.93	$\theta_{d12}$	60
	$Z_{t11}$	50	$\theta_{d21}$	45.5

TABLE II. ADMITTANCE  $Y_D$

Frequency	$Y_D$
2.1 GHz	$0.003294 + j0.001802$
2.9 GHz	$0.009929 + j0.019631$

TABLE III. ADMITTANCE  $Y_T$  AND  $Y_{T1}$

Frequency	$Y_T$	$Y_{T1}$
2.9 GHz	$0.001211 + j0.010543$	$0.02 + j0.08750$

TABLE IV. DESIGN PARAMETERS OF QUAD-BAND SUSCEPTANCE

Impedance	value( $\Omega$ )	Electrical length	value( $^\circ$ )
$Z_{1t}$	60	$\theta_1$	$90 @ f_1$
$Z_{2t}$	60	$\theta_2$	$45 @ f_1$
$Z_{3t}$	60	$\theta_3$	$68.91 @ f_1$
$Z_{1s}$	100	$\theta_{1s}$	$90 @ f_1$
$Z_{2s}$	100	$\theta_{2s}$	$90 @ f_2$
$Z_{3s}$	100	$\theta_{3s}$	$90 @ f_3$
$Z_{4t} = Z_{4s}$	60	$\theta_{4T}$	$14.09 @ f_1$

A transmission line of  $50 \Omega$  is therefore added from the source side whose electrical length,  $\theta$ , can be found using tuning feature available in the Keysight ADS to get the input impedance equal to  $50 \Omega$ . Alternatively, formula of input impedance could also be invoked to find the electrical analytically as follows:

$$Y_A = \frac{1}{Z_0} * \frac{Z_0 + j(1/Y_T) * \tan \theta}{(1/Y_T) + jZ_0 * \tan \theta} \quad (6)$$

$$\text{Re}(Y_A) = 0.02 \quad (7)$$

The above equations can be solved to evaluate  $\theta$ . It must be noted that the value of  $Y_T$  in (6) corresponds to  $f_4$  and it can be read from Table III.

The electrical length of  $50 \Omega$  TL-section is calculated as  $\theta = 32.768^\circ @ f_1$ . Now, at the input of TL-section the impedance is matched at three frequencies while at fourth frequency the admittance ( $Y_{T1}$ ) is calculated and given in Table III. The imaginary part of  $Y_{T1}$  as given in Table III is used to design the quad-frequency stub is designed. More details of quad-frequency stub design can be obtained from [12]. The values of various line impedances and electrical lengths are tabulated in Table IV.

The following two points must be clear from above descriptions:

- 1) There is no limitation on the number of frequency bands. For example, extension to penta-frequency matching would require addition of a  $50 \Omega$  TL-section and a quad-to-penta-band transformer (QPBT). A QPBT can be designed as a special case of multi-frequency DC-feed outlined in [12].
- 2) There is no limitation on type of load. In fact, as pointed out in [9], the type of load depends on the type of the

DBIT used in multi-frequency matching network. If the DBIT could handle an FDCL, the multi-frequency matching network will work for FDCL. If the DBIT can work for a real load, the multi-frequency matching network will work for real loads.

## V. SIMULATION AND MEASUREMENT RESULTS

Based on the design example outlined in the previous section, a prototype is fabricated on the Rogers RO5880 substrate with  $\epsilon_r = 2.2$ ,  $\tan\delta = 0.0009$  and substrate thickness of 1.575mm. The copper cladding of the laminate is 35 $\mu$ m on both the sides.

The prototype is shown in Fig. 6. The final design is achieved after optimizations in the Keysight ADS simulation tool due to several junction discontinuities present in the design. The measurement results are compared with the EM simulations and are depicted in Fig. 7. It can be observed that the EM and measured results are in good agreement. A slight deviation on the response can be attributed to the optimizations done to address the discontinuities in the design, and due to anomaly in the resistor models.

A comparison of the proposed design technique with the previously reported designs is presented in Table V. It is apparent that the proposed scheme helps overcome many limitations of state-of-the-art designs.

## VI. CONCLUSION

A simple and systematic design approach to design a novel quad-frequency impedance transformer with closed form design equations is reported. The technique has been validate

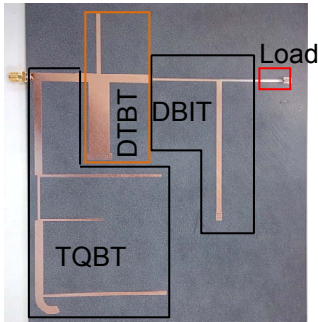


Fig. 6. The fabricated quad-frequency impedance transformer on RO5880.

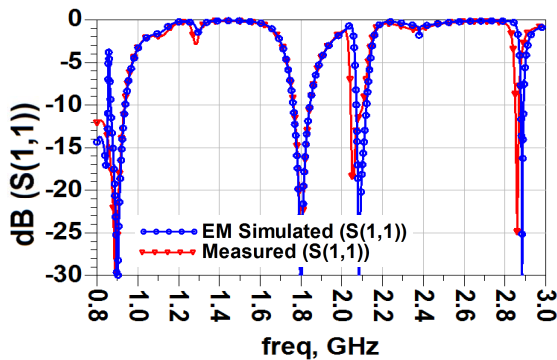


Fig. 7. EM simulated and measured return loss.

TABLE V. COMPARISON WITH PREVIOUS DESIGNS

Ref.	Frequency Bands	Type of Load	Lumped/Distributed
[3]	2	FDCL	Distributed
[8]	3	Real	Distributed
[9]	3	Both	Distributed
[10]	multi	FDCL	Lumped
[11]	multi	FDCL	Distributed
This Work	multi	Both	Distributed

through a prototype developed on RO5880 substrate. It can be said that this technique could be extended to penta-band or beyond by utilizing additional sections of L-networks. However, this will come at a price of increased board size. Moreover, there is no restriction on the type of load to be considered.

## REFERENCES

- [1] K. Rawat, M. S. Hashmi, and F. M. Ghannouchi, "Dual-band RF circuits and components for multi-standard software defined radios," *IEEE Circuits Syst. Mag.*, vol. 12, no. 1, pp. 12–32, Feb. 2012.
- [2] Y. Wu, L. Jiao and Y. Liu, "Comments on "novel dual-band matching network for effective design of concurrent dual-band power amplifiers,"" *IEEE Trans. Circuits Syst. I, Reg. Papers*, vol. 62, no. 9, pp. 2361–2361, Aug. 2015.
- [3] O. Manoochchri, A. Asodeh, and K. Forooghi, "Pi-model dual-band impedance transformer for unequal complex impedance loads," *IEEE Microw. Wireless Compon. Lett.*, vol.25, no.4, pp.238–240, Apr. 2015.
- [4] M. A. Maktoomi, M.S. Hashmi, and F. M. Ghannouchi, "A T-section dual-band matching network for frequency-dependent complex loads incorporating coupled line with dc-block property suitable for dual-band transistor amplifiers," *Prog. Electromagn. Res. C*, vol. 54, pp. 75–84, 2014.
- [5] M. A. Maktoomi and M. S. Hashmi, "A coupled-line based l-section de-isolated dual-band real to real impedance transformer and its application to a dual-band t-junction power divider," *Progr. Electromagn. Res. C*, vol. 55, pp. 95–104, 2014.
- [6] M. A. Nikravan and Z. Atlasbaf, "T-section dual-band impedance transformer for frequency-dependent complex impedance loads," *IET Electron. Lett.*, vol. 47, no. 9, pp. 551–553, April 2011.
- [7] Y. Wu, Y. Liu, and S. Li, "A compact Pi-structure dual band transformer," *Prog. in Electromagn. Res.*, vol. 88, pp. 121–134, 2008.
- [8] X. H. Wang, L. Zhang, Y. Xu, Y. F. Bai, C. Liu, and X.-W. Shi, "A tri-band impedance transformer using stubbed coupling line," *Prog. in Electromagn. Res.*, vol. 141, pp. 33–45, 2013.
- [9] M. A. Maktoomi, M. S. Hashmi, A. P. Yadav, and V. Kumar., "A generic tri-band matching network," *IEEE Microw. Wireless Compon. Lett.*, vol. 26, no. 5, May 2016.
- [10] N. Nallam and S. Chatterjee, "Multi-band frequency transformations, matching networks and amplifiers," *IEEE Trans. Circuits Syst. I, Reg. Papers*, vol. 60, no. 6, pp. 1635–1647, Jun. 2013.
- [11] Y. Liu, Y. Zhao, S. Liu, Y. Zhou, and Y. Chen, " Multi-frequency impedance transformers for frequency-dependent complex loads," *IEEE Trans. Microw. Theory Techn.*, vol. 61, no. 9, pp. 3225–3235, Sep. 2013.
- [12] M. A. Maktoomi, M. Akbarpour, M. S. Hashmi, and F. M. Ghannouchi, "A theorem for multi-frequency DC-feed network design," *IEEE Microw. Wireless Compon. Lett.*, 2016 (accepted).